COMPUTER RESEARCH AND MODELING
2024 VOL. 16 NO. 5 P. e1093–e1105
DOI: 10.20537/2076-7633-2024-16-5-1093-1105

Ки&М

NUMERICAL METHODS AND THE BASIS FOR THEIR APPLICATION

UDC: 532.5

Numerical simulation of the backward influence of a polymer additive on the Kolmogorov flow

V. V. Denisenko[1,a], S. V. Fortova[1], V. V. Lebedev[2], I. V. Kolokolov[2]

[1]Institute for Computer Aided Design of the RAS,
19/18 2nd Brestskaya st., Moscow, 123056, Russia
[2]L. D. Landay Institute for Theoretical Physics of the RAS,
1A Akademika Semenova av., Chernogolovka, Moscow region, 142432, Russia

E-mail: [a] ned13@rambler.ru

Received 19.07.2024, after completion — 16.08.2024.
Accepted for publication 03.09.2024.

A numerical method is proposed that approximates the equations of the dynamics of a weakly compressible viscous flow in the presence of a polymer component of the flow. The behavior of the flow under the influence of a static external periodic force in a periodic square cell is investigated. The methodology is based on a hybrid approach. The hydrodynamics of the flow is described by a system of Navier – Stokes equations and is numerically approximated by the linearized Godunov method. The polymer field is described by a system of equations for the vector of stretching of polymer molecules **R**, which is numerically approximated by the Kurganov – Tedmor method. The choice of model relationships in the development of a numerical methodology and the selection of modeling parameters made it possible to qualitatively model and study the regime of elastic turbulence at low Reynolds $\mathrm{Re} \sim 10^{-1}$. The polymer solution flow dynamics equations differ from the Newtonian fluid dynamics equations by the presence on the right side of the terms describing the forces acting on the polymer component part. The proportionality coefficient A for these terms characterizes the backward influence degree of the polymers number on the flow. The article examines in detail how the flow and its characteristics change depending on the given coefficient. It is shown that with its growth, the flow becomes more chaotic. The flow energy spectra and the spectra of the polymers stretching field are constructed for different values of A. In the spectra, an inertial sub-range of the energy cascade is traced for the flow velocity with an indicator $k \sim -4$, for the cascade of polymer molecules stretches with an indicator -1.6.

Keywords: numerical modeling, elastic turbulence, hydrodynamic instability

Citation: *Computer Research and Modeling*, 2024, vol. 16, no. 5, pp. e1093–e1105 (Russian).

The work of V. V. Denisenko and S. V. Fortova was performed within the framework of the ICAD RAS state assignment, No. 124022400174-3, V. V. Lebedev work with the support of the Russian Science Foundation, grant No. 23-72-30006, I. V. Kolokolov work within the framework of the ITP RAS State Assignment, No. 075-15-2019-1893.

КОМПЬЮТЕРНЫЕ ИССЛЕДОВАНИЯ
И МОДЕЛИРОВАНИЕ 2024 Т. 16 № 5 С. e1093–e1105
DOI: 10.20537/2076-7633-2024-16-5-1093-1105

Ки&М

ЧИСЛЕННЫЕ МЕТОДЫ И ОСНОВЫ ИХ РЕАЛИЗАЦИИ

УДК: 532.5

Численное моделирование обратного влияния полимерной примеси на колмогоровское течение

В. В. Денисенко[1,a], С. В. Фортова[1], В. В. Лебедев[2], И. В. Колоколов[2]

[1]Институт автоматизации проектирования РАН,
Россия, 123056, г. Москва, ул. 2-я Брестская, д. 19, стр. 18
[2]Институт теоретической физики имени Л. Д. Ландау РАН,
Россия, 142432, Московская область, г. Черноголовка, пр-т Академика Семёнова, д. 1а

E-mail: [a] ned13@rambler.ru

Получено 19.07.2024, после доработки — 16.08.2024.
Принято к публикации 03.09.2024.

Предложен численный метод, аппроксимирующий уравнения динамики слабосжимаемого вязкого течения при наличии полимерной составляющей потока. Исследуется поведение течения под воздействием статической внешней периодической силы в периодической квадратной ячейке. Методика основывается на гибридном подходе. Гидродинамика течения описывается системой уравнений Навье – Стокса и численно аппроксимируется линеаризованным методом Годунова. Полимерное поле описывается системой уравнений для вектора растяжений полимерных молекул **R**, которая численно аппроксимируются методом Курганова – Тедмора. Выбор модельных соотношений при разработке численной методики и подбор параметров моделирования позволили на качественном уровне смоделировать и исследовать режим эластической турбулентности при низких числах Рейнольдса $\mathrm{Re} \sim 10^{-1}$. Уравнения динамики течения полимерного раствора отличаются от уравнений динамики ньютоновской жидкости наличием в правой части членов, описывающих силы, действующие со стороны полимерной компоненты. Коэффициент пропорциональности A при данных членах характеризует степень обратного влияния количества полимеров на поток. В статье подробно исследуется влияние этого коэффициента на структуру и характеристики потока. Показано, что с его ростом течение становится более хаотическим. Построены энергетические спектры полученных течений и спектры полей растяжения полимеров для различных величин коэффициента A. В спектрах прослеживается инерциальный поддиапазон энергетического каскада для скорости течения с показателем $k \sim -4$, для каскада растяжений полимерных молекул с показателем $-1{,}6$.

Ключевые слова: численное моделирование, эластическая турбулентность, гидродинамическая неустойчивость

Работа В. В. Денисенко и С. В. Фортовой выполнена в рамках Госзадания ИАП РАН, № 124022400174-3, работа В. В. Лебедева — при поддержке Российского научного фонда, грант № 23-72-30006, работа И. В. Колоколова — в рамках Госзадания ИТФ РАН, № 075-15-2019-1893.

1. Introduction

The addition of polymeric molecules to a fluid flow leads to a radical change in the dynamics of its flow. Laboratory experiments show that the presence of even a small concentration of polymers can significantly change the properties of laminar $\mathrm{Re} \ll 1$ flows and create a new form of turbulence called elastic turbulence. For Newtonian fluid flow, the transition to turbulence is determined by the Reynolds number Re. The higher Re, the more unstable the flow becomes, which leads to the emergence and development of a turbulent flow regime. However, in a fluid with polymeric molecules present, a so-called viscoelastic effect occurs due to the presence of another nonlinear term characterizing the effect of polymeric molecules on the flow. The influence of the polymer additive on the flow is described by another dimensionless parameter, the Weissenberg number $\mathrm{Wi} = \frac{U}{\gamma_0 L}$, defined by the multiplication of the characteristic gradient of the fluid flow velocity $\frac{U}{L}$ and the relaxation time of the polymer molecule to its equilibrium state $\frac{1}{\gamma_0}$. As physical experiments show, the emergence and development of flow instability at low $\mathrm{Re} \ll 1$ values occur precisely due to the presence of these elastic forces characterized by $\mathrm{Wi} \gg 1$ [Steinberg, 2021; Shahmardi et al., 2019; Belan, Chernykh, Lebedev, 2018; Hong-Na et al., 2013].

Although the phenomenon of elastic turbulence was discovered only two decades ago, its application has already become possible in various fields such as the efficient mixing of viscous fluids, in particular in curved microchannels at $\mathrm{Re} \ll 1$ [Groisman, Steinberg, 2001; Burghelea et al., 2004; Gan, Lam, Nguyen, 2006] and, consequently, for heat transfer enhancing in microchannels [Traore, Castelain, Burghelea, 2015; Whalley et al., 2015; Abed et al., 2016; Li et al., 2017]. In addition, effective emulsification of oil droplets and breaking capillary effect were observed [Slutsky, Steinberg, 2005; Poole et al., 2012], but, first of all, a significant intensification of crude oil production compared to conventional chemical flooding was established [Clarke et al., 2015; Howe, Clarke, Giernalczyk, 2015; Mitchell et al., 2016]. As in the case of hydrodynamic turbulence, the properties of elastic turbulence depend significantly on the boundary conditions. In this article, we will not consider the solid wall issue, restricting ourselves to the two-dimensional periodic case.

Numerical modeling of the elastic turbulence phenomenon is quite a sophisticated challenge. In numerical modeling of the polymer component, polymer models such as Oldroyd-B [Oldroyd, 1950] and FENE-P [Peterlin, 1961] are mainly used. The primary problem of numerical modeling with any of these models is numerical instability arising [Alves, Oliveira, Pinho, 2021]. Excessive stretching of polymer molecules, occurring at large values of Wi, characteristic of elastic turbulence, leads to steep stress gradients in the polymer field, which can lead to instability of the numerical calculation. These numerical instabilities can be partially addressed by using high-resolution discretization schemes [Kurganov, Tadmor, 2000; Vaithianathan et al., 2006], following strict polymer requirements [Vaithianathan, Collins, 2003], and adding an artificial diffusion rate to the constitutive equations per polymer component [Thomases, Shelley, Thiffeault, 2011; Gupta, Vincenzi, 2019].

However, since the elastic turbulence regime is driven solely by elastic instabilities, the artificial diffusion rate can significantly affect the numerical solution, which may lead to an incorrect physical interpretation of the chaotic regime [Gupta, Vincenzi, 2019]. In some cases, these numerical stability problems can be partially eliminated by the local application of artificial diffusion only in regions with steep stretching gradients of the polymer [Dubief et al., 2005].

Thus, at this stage of the study, the task arises of developing a numerical model that could demonstrate the effects of elastic turbulence at a qualitative level. It should be emphasized here that we do not set the task of obtaining results that could be used as the basis for describing real experiments on elastic turbulence. This formulation determined the choice of model relations in the development of numerical methods, as well as the selection of modeling parameters. This makes it possible to circumvent the difficulties described above that arise in numerical modeling. The paper

uses a numerical technique of the second order of accuracy [Годунов и др., 2020; Kurganov, Tadmor, 2000], constructed for direct numerical simulation of the dynamics of weakly compressible viscous flows in the presence of structural components in them. Using this technique, the flow of the model medium is numerically studied at $\mathrm{Re} \sim 10^{-1}$ in the presence of an external periodic force. The instability of such a flow was obtained and the influence of polymers on the flow and its energy characteristics was studied.

2. Problem statement. Model equations

The equations of the dynamics of the flow of a polymer solution differ from the equations of the dynamics of a Newtonian fluid by the presence on the right side of the terms describing the forces acting on the part of the polymer component. The proportionality coefficient A for these terms characterizes the degree of backward influence of polymers on the flow.

Consider the polymer component of the flow as a structural component to the hydrodynamic flow in the form of deformable polymer molecules. The deformation is characterized by a vector $\mathbf{R}$ (R^x, R^y are the components of the vector $\mathbf{R}$ on the OX and OY axes), which determines the direction in which the boundary of the molecular phase changes. Let's write down a system of model equations describing the dynamics of a weakly compressible viscous flow involving a structural component. It consists of a system of Navier – Stokes equations for the hydrodynamic phase of the flow and equations describing the dynamics of stretching of the polymer component of the flow $\mathbf{R}$ [Steinberg, 2021; Денисенко, Фортова, 2023]:

$$
\begin{gathered}
\frac{\partial \rho}{\partial t} + \nabla \cdot (\rho \mathbf{V}) = 0, \\
\frac{\partial \rho u}{\partial t} + \nabla \cdot (\rho u \mathbf{V}) = -\frac{\partial p}{\partial x} - \rho G \sin(ky)\cos(kx) + \mu \Delta u + A\frac{\partial}{\partial x}\left(\gamma(R)\{R^x\}^2\right) + A\frac{\partial}{\partial y}\left(\gamma(R) R^x R^y\right), \\
\frac{\partial \rho v}{\partial t} + \nabla \cdot (\rho v \mathbf{V}) = -\frac{\partial p}{\partial y} + \rho G \sin(kx)\cos(ky) + \mu \Delta v + A\frac{\partial}{\partial y}\left(\gamma(R)\{R^y\}^2\right) + A\frac{\partial}{\partial x}\left(\gamma(R) R^x R^y\right), \\
\frac{\partial\left(\frac{\rho \mathbf{V}^2}{2} + e\right)}{\partial t} + \nabla \cdot \left(\mathbf{V}\left(\frac{\rho \mathbf{V}^2}{2} + p + e\right)\right) = \frac{\partial}{\partial x}\left(\mu u \rho\left(\frac{\partial u}{\partial x} - \frac{\partial v}{\partial y}\right) + Au\gamma(R)\left(R^x\right)^2 + \right. \\
+ v\mu\rho\left(\frac{\partial v}{\partial x} + \frac{\partial u}{\partial y}\right) + Av\gamma(R) R^x R^y\Big) + \frac{\partial}{\partial y}\left(\mu u \rho\left(\frac{\partial u}{\partial y} + \frac{\partial v}{\partial x}\right) + Au\gamma(R) R^x R^y + \right. \\
\left. + \mu v \rho\left(\frac{\partial v}{\partial y} - \frac{\partial u}{\partial x}\right) + Av\gamma(R)\left(R^y\right)^2\right) - u\rho G \sin(ky)\cos(kx) + v\rho G \sin(kx)\cos(ky), \\
\frac{\partial R^x}{\partial t} + u\frac{\partial R^x}{\partial x} + v\frac{\partial R^x}{\partial y} - R^x\frac{\partial u}{\partial x} - R^y\frac{\partial u}{\partial y} + \gamma(R) R^x = C_d \Delta R^x, \\
\frac{\partial R^y}{\partial t} + u\frac{\partial R^y}{\partial x} + v\frac{\partial R^y}{\partial y} - R^x\frac{\partial v}{\partial x} - R^y\frac{\partial v}{\partial y} + \gamma(R) R^y = C_d \Delta R^y, \\
e = \frac{3p}{2\rho}, \quad \gamma(R) = \gamma_0\left(1 + \frac{R^2}{R_m^2}\right), \quad \mathbf{V} = (u, v)^T.
\end{gathered}
\tag{1}
$$

Here, A stands for the coefficient proportional to the concentration of polymer molecules in the solution and characterizing the degree of inverse effect of polymer molecules on the flow, C_d stands for the artificial polymer diffusion coefficient introduced to stabilize the numerical solution, $\gamma(R)$ is the relaxation model of the polymer molecule, and G is the intensity of the external force. The nonlinear approximation

$$
\gamma(R) = \gamma_0\left(1 + \frac{R^2}{R_m^2}\right)
$$

was used as a model of polymer elasticity. Here R_m stands for the maximum amount of stretching of the polymer molecule. Under the condition $R \ll R_m$, we deal with the linear regime corresponding to the Oldroyd-B model [Oldroyd, 1950].

The system of equations is closed using the equation of state of an ideal gas $e = \frac{3p}{2\rho}$, where e is the volume density of the internal energy [Ландау, Лифшиц, 1986].

The flow parameters at the initial moment of time and the boundary conditions were chosen from considerations of stability of the numerical experiment. The values of the velocity components u, v at the initial moment of time were assumed to be zero, which corresponds to an undisturbed flow. The values of density and pressure were assumed to be equal:

$$\rho(x,\, y,\, t = 0) = 10 \text{ kg/m}^3; \quad p(x,\, y,\, t = 0) = 10^3 \text{ Pa}.$$

The initial stretching values of polymer molecules are as follows:

$$R^x(x,\, y,\, t = 0) = 0.2\cos(a_x x) \text{ m}; \quad R^y(x,\, y,\, t = 0) = 0.2\cos(a_y y) \text{ m};$$
$$a_x = 1 \text{ m}^{-1}; \quad a_y = 1 \text{ m}^{-1}.$$

The artificial diffusion rate C_d was chosen empirically, based on the requirements of stable numerical calculation and the ratio $\sqrt{\frac{C_d}{\gamma_0}} \sim h$, where h is the characteristic cell size of the computational grid. The intensity of the external force was assumed to be $G = 10^{-2}$ N/kg, the frequency of external periodic force $k = 2 \text{ m}^{-1}$. The relaxation coefficient of the polymer molecule was assumed to be $\gamma_0 = 10^{-6} \text{ s}^{-1}$ so $C_d = 10^{-9} \text{ m}^2/\text{s}$. The magnitude of dynamic viscosity $\mu = 0.5 \text{ Pa} \cdot \text{s}$. The A value ranged in $A = 50 \div 5 \cdot 10^6 \text{ kg}/\left(\text{m}^3 \cdot \text{s}\right)$. The computational domain is a square with sides $L \times L = 2\pi \times 2\pi$ m×m on the boundary of which periodic boundary conditions are set and is covered by a uniform computational grid of mesh dimension 250×250.

3. Numerical method

For the numerical approximation of system (1), a combination of two numerical techniques — the linearized Godunov method [Годунов и др., 2020] and the Kurganov – Tadmor method [Kurganov, Tadmor, 2000] were used. The linearized Godunov method was used to approximate the hydrodynamic part of the model — Navier – Stokes equations, and the equations describing the polymer part were approximated with the Kurganov – Tadmore method. It should be noted that the choice of the linearized Godunov scheme for calculating the hydrodynamic part of the flow is due to the existence of large gradients of flow parameters when an elastic turbulence regime occurs. Let's briefly describe the numerical method.

Let's write down the system of Navier – Stokes equations in a divergent form:

$$\begin{pmatrix} \rho \\ \rho u \\ \rho v \\ \frac{\rho \mathbf{V}^2}{2} + e \end{pmatrix}_t + \begin{pmatrix} \rho u \\ \rho u^2 + p \\ \rho uv \\ u\left(\frac{\rho u^2}{2} + p + e\right) \end{pmatrix}_x + \begin{pmatrix} \rho v \\ \rho uv \\ \rho v^2 + p \\ v\left(\frac{\rho u^2}{2} + p + e\right) \end{pmatrix}_y = \mu \begin{pmatrix} 0 \\ \frac{\partial u}{\partial x} \\ \frac{\partial v}{\partial x} \\ u\rho\left(\frac{\partial u}{\partial x} - \frac{\partial v}{\partial y}\right) + v\rho\left(\frac{\partial v}{\partial x} + \frac{\partial u}{\partial y}\right) \end{pmatrix}_x +$$
$$+ \mu \begin{pmatrix} 0 \\ \frac{\partial u}{\partial y} \\ \frac{\partial v}{\partial y} \\ u\rho\left(\frac{\partial u}{\partial y} + \frac{\partial v}{\partial x}\right) + v\rho\left(\frac{\partial v}{\partial y} - \frac{\partial u}{\partial x}\right) \end{pmatrix}_y + A\gamma(R) \begin{pmatrix} 0 \\ (R^x)^2 \\ R^x R^y \\ u(R^x)^2 + vR^x R^y \end{pmatrix}_x + A\gamma(R) \begin{pmatrix} 0 \\ R^x R^y \\ (R^y)^2 \\ uR^x R^y + v(R^y)^2 \end{pmatrix}_y.$$

Viscous and "polymer" flows through the faces of the cells of the computational grid are calculated by the usual averaging.

Convective flows

$$\begin{pmatrix} \rho u \\ \rho u^2 + p \\ \rho uv \\ u\left(\frac{\rho u^2}{2} + p + e\right) \end{pmatrix}, \quad \begin{pmatrix} \rho v \\ \rho uv \\ \rho v^2 + p \\ v\left(\frac{\rho u^2}{2} + p + e\right) \end{pmatrix}$$

are calculated using the linearized Godunov method as follows:

$$P^{n+1/2}_{i+1/2,j} = \frac{\frac{p^n_{i,j}}{\rho^n_{i,j}c^n_{i,j}} + \frac{p^n_{i+1,j}}{\rho^n_{i+1,j}c^n_{i+1,j}} + u^n_{i,j} - u^n_{i+1,j}}{\frac{1}{\rho^n_{i,j}c^n_{i,j}} + \frac{1}{\rho^n_{i+1,j}c^n_{i+1,j}}}; \quad U^{n+1/2}_{i+1/2,j} = \frac{\rho^n_{i,j}c^n_{i,j}u^n_{i,j} + \rho^n_{i+1,j}c^n_{i+1,j}u^n_{i+1,j} + p^n_{i,j} - p^n_{i+1,j}}{\frac{1}{\rho^n_{i,j}c^n_{i,j}} + \frac{1}{\rho^n_{i+1,j}c^n_{i+1,j}}};$$

$$V^{n+1/2}_{i+1/2,j} = \begin{cases} v^n_{i,j}, & U^{n+1/2}_{i+1/2,j} \geqslant 0, \\ v^n_{i+1,j}, & U^{n+1/2}_{i+1/2,j} < 0, \end{cases} \quad R^{n+1/2}_{i+1/2,j} = \begin{cases} \rho^n_{i,j}\left(1 - \frac{U^{n+1/2}_{i+1/2,j} - u^n_{i,j}}{c^n_{i,j}}\right), & U^{n+1/2}_{i+1/2,j} \geqslant 0, \\ \rho^n_{i+1,j}\left(1 - \frac{u^n_{i+1,j} - U^{n+1/2}_{i+1/2,j}}{c^n_{i+1,j}}\right), & U^{n+1/2}_{i+1/2,j} < 0. \end{cases}$$

Here P, U, V, R are the pressure flows, the velocity and density components, respectively. Half-integer indexes indicate flows on the faces of cells, integers indicate the values of the values in the center of the cell.

Next, we describe the approximation of the equations to the polymer stretching vector **R**. Let us write the equations of the system (1) for the polymer stretch vector in divergent form:

$$\begin{pmatrix} R^x \\ R^y \end{pmatrix}_t + \begin{pmatrix} uR^x \\ uR^y \end{pmatrix}_x - \begin{pmatrix} C_d\frac{\partial R^x}{\partial x} \\ C_d\frac{\partial R^y}{\partial x} \end{pmatrix}_x + \begin{pmatrix} vR^x \\ vR^y \end{pmatrix}_y - \begin{pmatrix} C_d\frac{\partial R^x}{\partial y} \\ C_d\frac{\partial R^y}{\partial y} \end{pmatrix}_y = \begin{pmatrix} 2R^x\frac{\partial u}{\partial x} + R^y\frac{\partial u}{\partial y} + R^x\frac{\partial v}{\partial x} - \gamma(R)R^x \\ R^x\frac{\partial v}{\partial x} + 2R^y\frac{\partial v}{\partial y} + R^y\frac{\partial u}{\partial x} - \gamma(R)R^y \end{pmatrix}.$$

The main principle of the Kurganov – Tadmore technique implies the calculation of convective fluxes

$$\begin{pmatrix} uR^x \\ uR^y \end{pmatrix}, \quad \begin{pmatrix} vR^x \\ vR^y \end{pmatrix}$$

on the faces of computational cells, and for approximation of other terms (diffusion and source), the usual averaging on the faces of computational grid cells is applied. Let us denote the convective flux along the axes x, y:

$$F = \begin{pmatrix} uR^x \\ uR^y \end{pmatrix}; \quad G = \begin{pmatrix} vR^x \\ vR^y \end{pmatrix},$$

vector-column of unknowns

$$R = \begin{pmatrix} R^x \\ R^y \end{pmatrix}.$$

Convective fluxes will then be calculated as follows:

$$F^n_{i+1/2,j} = \frac{F\left(\left(R^+_{i+1/2,j}\right)^n\right) + F\left(\left(R^-_{i-1/2,j}\right)^n\right)}{2} - \frac{\left(a^x_{i+1/2,j}\right)^n}{2}\left(\left(R^+_{i+1/2,j}\right)^n - \left(R^-_{i-1/2,j}\right)^n\right);$$

$$G^n_{i,j+1/2} = \frac{G\left(\left(R^+_{i,j+1/2}\right)^n\right) + G\left(\left(R^-_{i,j-1/2}\right)^n\right)}{2} - \frac{\left(a^y_{i,j+1/2}\right)^n}{2}\left(\left(R^+_{i,j+1/2}\right)^n - \left(R^-_{i,j-1/2}\right)^n\right);$$

$$\left(R^\pm_{i+1/2,j}\right)^n = R^n_{i+1,j} \mp \frac{\Delta x}{2}(R_x)^n_{i+1/2\pm1/2,j}; \quad \left(R^\pm_{i,j+1/2}\right)^n = R^n_{i,j+1} \mp \frac{\Delta y}{2}(R_y)^n_{i,j+1/2\pm1/2};$$

$$\left(a^x_{i+1/2,j}\right)^n = \max_\pm\left(\frac{\partial F}{\partial R}\left(\left(R^\pm_{i+1/2,j}\right)^n\right)\right) = \left|u_{i+1/2,j}\right|; \quad \left(a^y_{i+1/2,j}\right)^n = \max_\pm\left(\frac{\partial G}{\partial R}\left(\left(R^\pm_{i,j+1/2}\right)^n\right)\right) = \left|v_{i+1/2,j}\right|;$$

$$u_{i+1/2,j} = \frac{1}{2}(u_{i,j} + u_{i+1,j}); \quad v_{i+1/2,j} = \frac{1}{2}(v_{i,j} + v_{i+1,j});$$

$$(R_x)^n_{i,j} = \min \mathrm{mod}\left(\theta\frac{(R_x)^n_{i,j} - (R_x)^n_{i-1,j}}{\Delta x}, \frac{(R_x)^n_{i+1,j} - (R_x)^n_{i-1,j}}{2\Delta x}, \theta\frac{(R_x)^n_{i+1,j} - (R_x)^n_{i,j}}{\Delta x}\right);$$

$$(R_y)^n_{i,j} = \min \mathrm{mod}\left(\theta\frac{(R_y)^n_{i,j} - (R_y)^n_{i,j-1}}{\Delta y}, \frac{(R_y)^n_{i,j+1} - (R_y)^n_{i,j-1}}{2\Delta y}, \theta\frac{(R_y)^n_{i,j+1} - (R_y)^n_{i,j}}{\Delta y}\right);$$

$\theta = 1.5$ is a constraint weight ratio.

Here, semi-integer indices denote the fluxes on the cell faces, integer indices denote the values of the variables in the cell center, u, v stand for the x- and y-components of the flow velocity, and a is the local velocity of disturbance propagation. A minmod constraint was used to limit the slopes of the reconstructed solution in the cell.

4. Results of numerical modeling

Figire 1 shows the flow vorticity patterns at the same moment of time $t \sim 630$ s for different values of the A parameter. In all of the above, the value of the Reynolds number is $\mathrm{Re} \sim 10^{-1}$ and the Weissenberg number is $\mathrm{Wi} \sim 1000$. Figure 1 show the flow becomes more and more chaotic as A increases. Figures 2, 3 show the flow velocity patterns with flow lines and polymer stretching patterns $R = \sqrt{(R^x)^2 + (R^y)^2}$ respectively. Indeed, the magnitude of stretching R decreases with A increasing, which is explained by the increase in the inverse effect of polymer molecules on the flow, due to which it becomes chaotic. This dependence suggests that the chaotic flow occurs due to an increase in the reverse effect of the polymer component on the flow.

The emergence of instabilities in solution flow comes from the regions of the greatest stretching of polymers, i. e., the region of flow hyperbolicity. The flow resulting from the external force is vortical; in the regions between vortices, the flow is hyperbolic, and the degree of stretching of polymer molecules is the highest here. The reverse effect of highly stretched polymers on the flow leads to instabilities and their further development.

Figure 4 shows the velocity $E_v(k)$ (left) and stretching spectra of the polymer molecules $E_r(k)$ (right) of the resulting flow at $t \sim 630$ s for different values of the A parameter. The spectra were

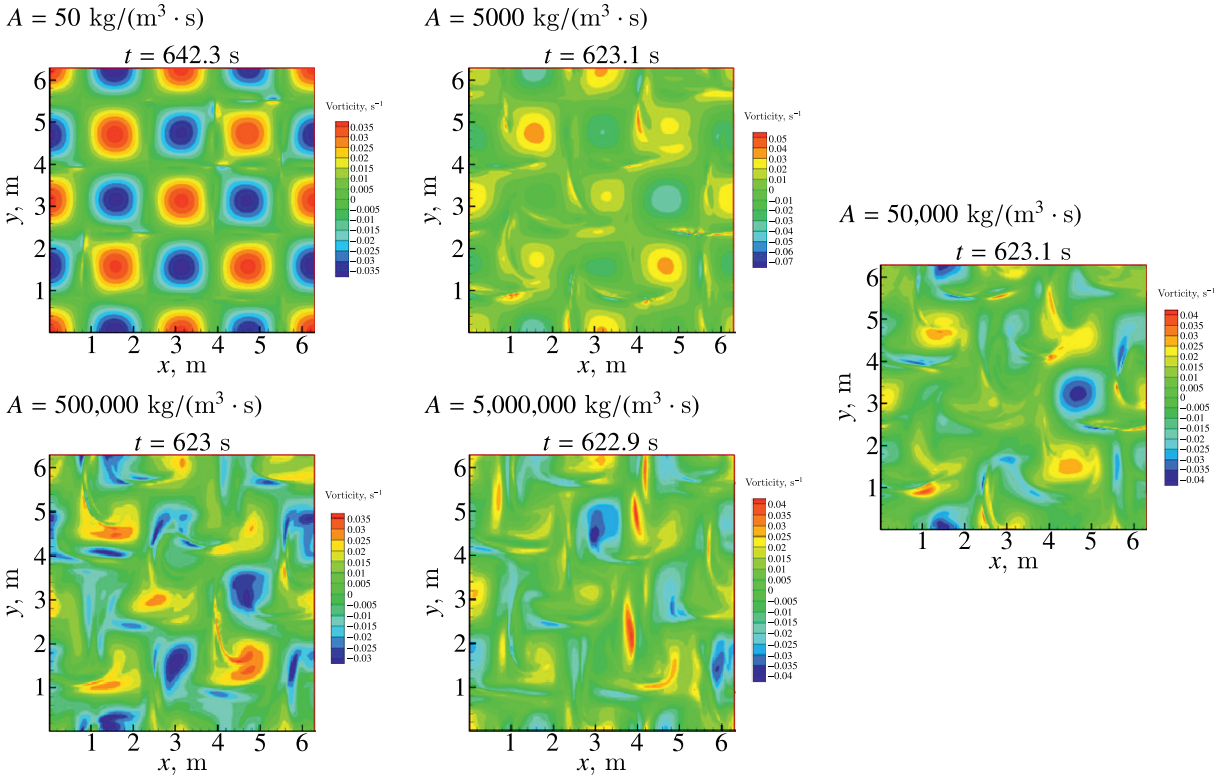

Рис. 1. Vorticity fields of the polymer solution flow in a periodic cell under the influence of an external periodic force for different values of the parameter A characterizing the degree of reverse influence on the flow at a time $t \sim 630$ s

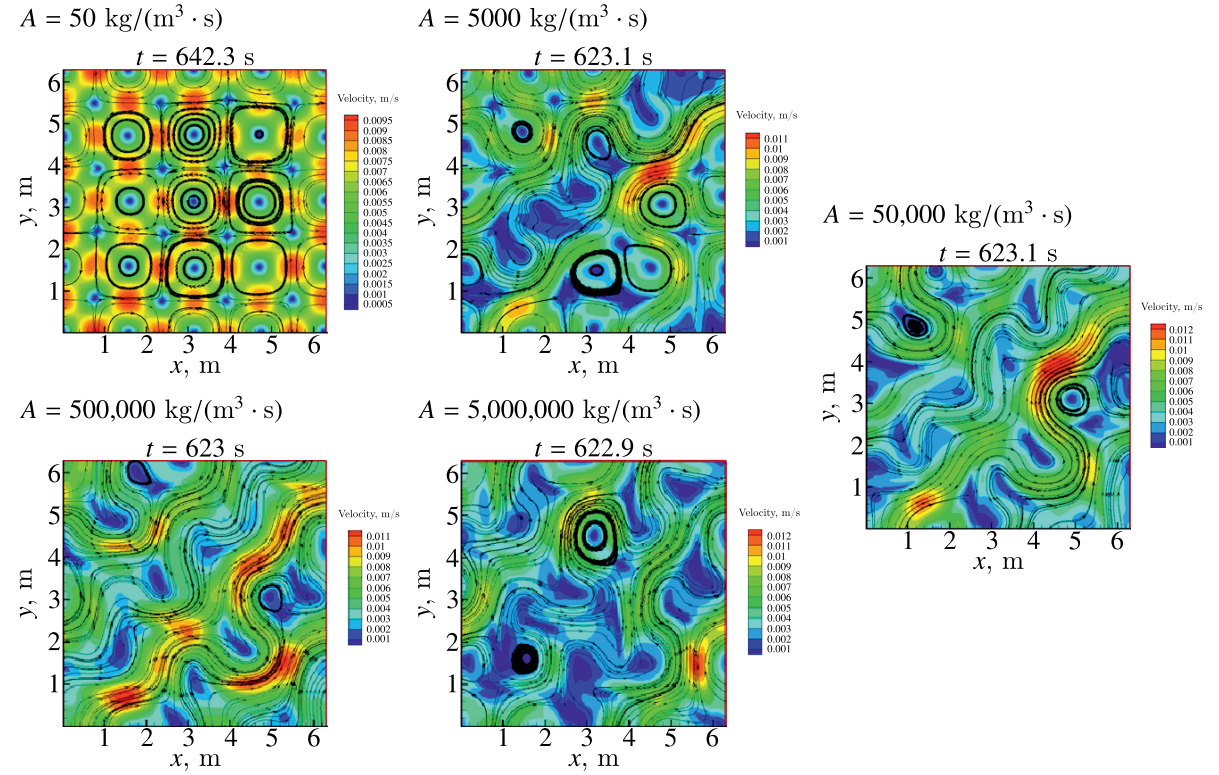

Рис. 2. The flow velocity fields of a polymer solution with current lines in a periodic cell, which is under the influence of an external periodic force for various values of the parameter characterizing the degree of reverse influence on the flow A, at a time $t \sim 630$ s

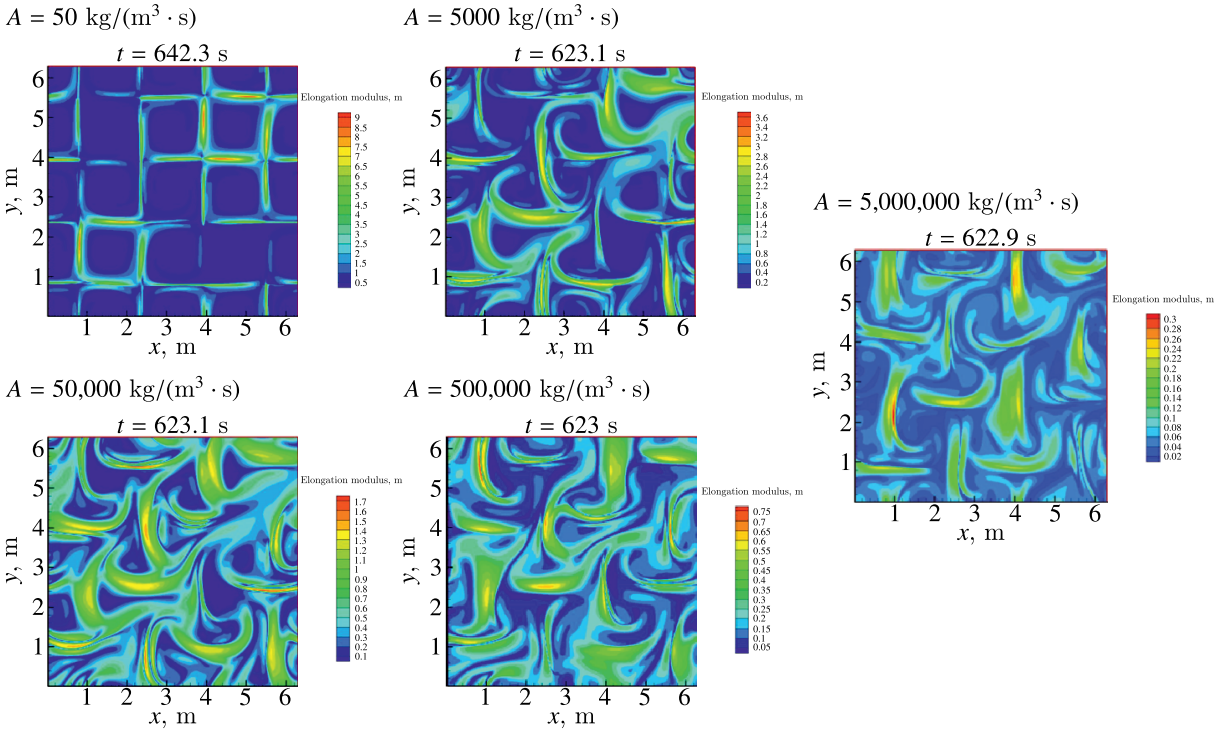

Рис. 3. Fields of the elongation modulus $R = \sqrt{(R^x)^2 + (R^y)^2}$ of polymer molecules in a periodic cell, which is under the influence of an external periodic force for various parameter values at a time $t \sim 630$ s

calculated as cosine-sine expansion:

$$E_v(k_x, k_y) = \sum_{i=0}^{1} \sum_{j=1}^{4} u^2_{i(j)}(k_x, k_y) + 2 \sum_{i=0}^{1} \left[u_{i(1)}(k_x, k_y) u_{i(2)}(k_x, k_y) + u_{i(3)}(k_x, k_y) u_{i(4)}(k_x, k_y) \right];$$

$$u_{i(1)}(k_x, k_y) = \frac{1}{\pi} \int_0^{2\pi} u_i(x, y) \cos(k_x x) \cos(k_y y)\, dx\, dy,$$

$$u_{i(2)}(k_x, k_y) = \frac{1}{\pi} \int_0^{2\pi} u_i(x, y) \cos(k_x x) \sin(k_y y)\, dx\, dy,$$

$$u_{i(3)}(k_x, k_y) = \frac{1}{\pi} \int_0^{2\pi} u_i(x, y) \sin(k_x x) \cos(k_y y)\, dx\, dy,$$

$$u_{i(4)}(k_x, k_y) = \frac{1}{\pi} \int_0^{2\pi} u_i(x, y) \sin(k_x x) \sin(k_y y)\, dx\, dy.$$

Here, the i index is introduced to number the axial velocity components (u, v). The resulting distribution in space (k_x, k_y) was averaged over the vector directions $\mathbf{k}$ in a ring of width $\delta = 0.5$:

$$E(k) = \sum_{k_x, k_y : \left| k - \sqrt{k_x^2 + k_y^2} \right| < \delta} E(k_x, k_y).$$

The stretching spectrum $E_r(k)$ was calculated similarly by $u \to R^x$, $v \to R^y$ substitution.

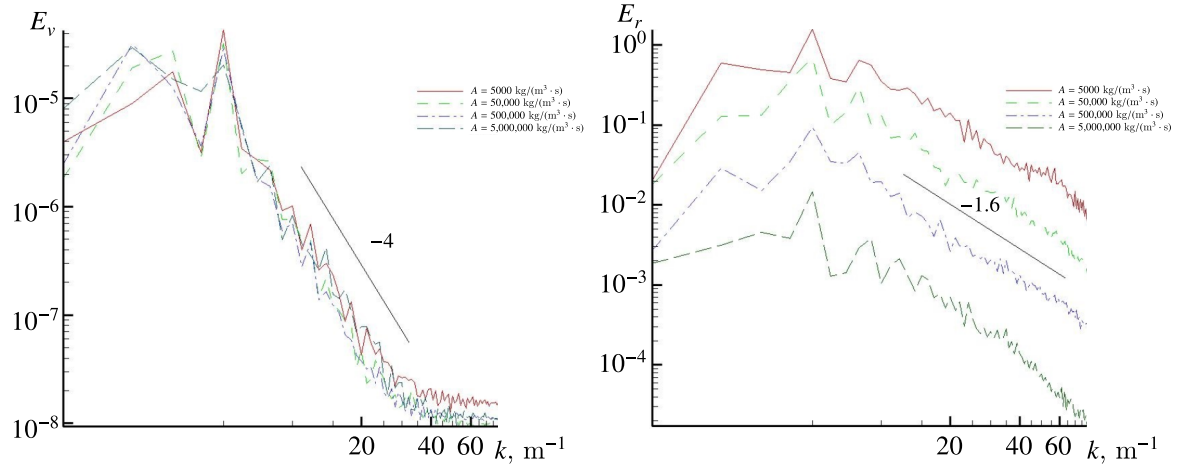

Рис. 4. The spectra of velocity E_v (left) and stretching of polymer molecules E_r (right) of chaotic flows of a polymer solution in a periodic cell under the influence of an external periodic force, depending on the value of the parameter A, plotted on a doubly logarithmic scale

As shown in Fig. 4, the spectral characteristics of the flow are practically independent of the A parameter, which determines the degree of the inverse influence of the polymer component of the solution on the flow itself. The inertial range of the energy cascade with the indicator -4 is clearly visible. For the stretching of polymer molecules, a dependence with the index -1.6 is observed. At the same time, as expected, with an increase in the parameter A, the energy of the polymer component of the flow decreases due to the transfer of polymer energy back into the flow.

From the results obtained, it can be concluded that the flow in Figs. 1–3 is in the regime of elastic turbulence, a chaotic flow caused by the presence of polymer additive.

5. Conclusion

The paper presents a numerical model that qualitatively demonstrates the emergence and development of an elastic turbulence regime — a chaotic flow of a medium containing a polymer component. Using the example of weakly compressible viscous flows of a polymer solution in a periodic square cell excited by an external force, flows with a low Reynolds number $\mathrm{Re} \sim 10^{-1}$ and a high Weissenberg number $\mathrm{Wi} \sim 1000$ are studied. With the determined model parameters, it is shown by numerical experiment that the presence of a polymer impurity significantly changes the nature of the hydrodynamic flow due to the influence of elastic forces acting from the polymer molecules. The action of these forces leads to a loss of stability of the hydrodynamic flow and the subsequent transition to the elastic turbulence regime. The instability of the flow occurs in areas of hyperbolicity, where the stretching of polymer molecules, and consequently their reverse effect on the flow, has a maximum value. It should be noted that the parameter characterizing the stability of such flows is a combination of Reynolds Re and Weissenberg Wi — the coefficient of elasticity $El = \frac{\mathrm{Wi}}{\mathrm{Re}}$ [Steinberg, 2021]. In the presented numerical experiments, this number was 10,000.

A hybrid numerical scheme of second-order accuracy approximating the polymer solution dynamics equations (1) is proposed to investigate the problem at hand. The hydrodynamic part of the system (1) — Navier – Stokes equations were approximated by the linearized Godunov method [Годунов и др., 2020], and the polymer part — by the Kurganov – Tadmor method [Kurganov, Tadmor, 2000].

The influence of the problem parameter characterizing the degree of inverse influence of elastic forces produced by deformed polymer molecules on the hydrodynamic flow A is investigated. As the

parameter A increases, the flow becomes more unstable and chaotic. The inertial range of the energy cascade with an indicator ~ -4 is obtained in the spectral characteristics of the flow. In the stretching spectra of polymer molecules, this indicator is equal to ~ -1.6. It is shown that the parameter A has the main effect on the stretching spectrum of polymer molecules. An increase in this parameter leads to a decrease in the energy contained in the polymer component of the flow and the transfer of polymer energy into the hydrodynamic flow.

List of designations

A — a coefficient proportional to the concentration of polymer molecules in solution and characterizing the degree of reverse influence of polymer molecules on the flow,
C_d — coefficient of artificial diffusion of polymers,
$\gamma(R)$ — relaxation model of a polymer molecule,
G — the intensity of the external force,
R_m — the maximum amount of a polymer molecule stretching,
e — internal energy volume density,
k — external periodic force frequency,
u — x-component of the solution flow velocity,
v — y-component of the solution flow velocity,
R^x — x-component of the polymer molecule stretching vector,
R^y — y-component of the polymer molecule stretching vector,
p — pressure,
ρ — solution density,
μ — dynamic viscosity,
Re — Reynolds number,
Wi — Weissenberg number,
γ_0 — relaxation model of the polymer molecule,
E_v — spectra of velocity,
E_r — spectra of stretching of polymer molecules,
$\mathbf{R}$ — the polymer molecule stretching vector.

Список литературы (References)

Годунов С. К., Денисенко В. В., Ключинский Д. В., Фортова С. В., Шепелев В. В. Исследование энтропийных свойств линеаризованной редакции метода Годунова // ЖВМиМФ. — 2020. — Т. 60, № 4. — С. 639–651.
Godunov S. K., Denisenko V. V., Klyuchinskii D. V., Fortova S. V., Shepelev V. V. Issledovanie entropiinykh svoistv linearizovannoi redaktsii metoda Godunova [Study of entropy properties of a linearized version of Godunov's method] // Computational Mathematics and Mathematical Physics. — 2020. — Vol. 60, No. 4. — P. 639–651 (in Russian).

Денисенко В. В., Фортова С. В. Численное моделирование эластической турбулентности в ограниченной двумерной ячейке // Сибирский журнал индустриальной математики. — 2023. — Т. 26, № 1. — С. 55–64.
Denisenko V. V., Fortova S. V. Chislennoe modelirovanie elasticheskoi turbulentnosti v ogranichennoi dvumernoi yacheike [Numerical simulation of elastic turbulence in a confined two-dimensional cell] // Siberian journal of Industrial Mathematics. — 2023. — Vol. 26, No. 1. — P. 55–64 (in Russian).

Ландау Л. Д., Лифшиц Е. М. Теоретическая физика: т. VI. Гидродинамика. — 3-е изд., перераб. — М.: Наука, Гл. ред. физ-мат. лит., 1986.
Landau L. D., Lifshitz E. M. Teoreticheskaya fizika: Vol. VI. Gidrodinamika [Theoretical physics: Vol. VI. Gydrodynamics]. — 3-e izd., pererab. — Moscow: Nauka, Gl. red. fiz-mat. lit., 1986 (in Russian).

Abed W. M., Whalley R. D., Dennis D. J. C., Poole R. J. Experimental investigation of the impact of elastic turbulence on heat transfer in a serpentine channel // J. Non-Newton. Fluid Mech. — 2016. — Vol. 231. — P. 68–78.

Alves M. A., Oliveira P. J., Pinho F. T. Numerical methods for viscoelastic fluid flows // Annu. Rev. Fluid Mech. — 2021. — Vol. 53. — P. 509–541.

Belan S., Chernykh A., Lebedev V. Boundary layer of elastic turbulence // J. Fluid Mech. — 2018. — Vol. 855. — P. 910–921.

Burghelea T., Segre E., Bar-Joseph I., Groisman A., Steinberg V. Chaotic flow and efficient mixing in a microchannel with a polymer solution // Phys. Rev. E. — 2004. — Vol. 69. — P. 066305.

Clarke A., Howe A. M., Mitchell J., Staniland J., Hawkes L., Leepera K. Mechanism of anomalously increased oil displacement with aqueous viscoelastic polymer solutions // Soft Matter. — 2015. — Vol. 11. — P. 3536–3541.

Dubief Y., Terrapon V. E., White C. M., Shaqfeh E. S. G., Moin P., Lele S. K. New answers on the interaction between polymers and vortices in turbulent flows // Flow Turbul. Combust. — 2005. — Vol. 74. — P. 311–329.

Gan H. Y., Lam Y. C., Nguyen N.-T. Polymer-based device for efficient mixing of viscoelastic fluids // Appl. Phys. Lett. — 2006. — Vol. 88. — P. 224103.

Groisman A., Steinberg V. Stretching of polymers in a random three-dimensional flow // Phys. Rev. Lett. — 2001. — Vol. 86. — P. 934–937.

Gupta A., Vincenzi D. Effect of polymer-stress diffusion in the numerical simulation of elastic turbulence // J. Fluid Mech. — 2019. — Vol. 870. — P. 405–418.

Hong-Na Z., Feng-Chen L., Yang C., Tomoaki K., Bo Y. Direct numerical simulation of elastic turbulence and its mixing-enhancement effect in a straight channel flow // Chin. Phys. B. — 2013. — Vol. 22, No. 2. — P. 024703.

Howe A. M., Clarke A., Giernalczyk D. Flow of concentrated viscoelastic polymer solutions in porous media: effect of $M(W)$ and concentration on elastic turbulence onset in various geometries // Soft Matter. — 2015. — Vol. 11. — P. 6419–6431.

Kurganov A., Tadmor E. New high-resolution central schemes for nonlinear conservation laws and convection – diffusion equations // Journal of Computational Physics. — 2000. — Vol. 160. — P. 241–282.

Li D.-Y., Li X.-B., Zhang H.-N., Li F.-C., Qian S., Joo S. W. Efficient heat transfer enhancement by elastic turbulence with polymer solution in a curved microchannel // Microfluid. Nanofluid. — 2017. — Vol. 21. — P. 10.

Mitchell J., Lyons K., Howe A. M., Clarke A. Viscoelastic polymer flows and elastic turbulence in three-dimensional porous structures // Soft Matter. — 2016. — Vol. 12. — P. 460–468.

Oldroyd J. G. On the formulation of rheological equations of state // Proc. R. Soc. Lond. Ser. A Math. Phys. Sci. — 1950. — Vol. 200. — P. 523–541.

Peterlin A. Streaming birefringence of soft linear macromolecules with finite chain length // Polymer. — 1961. — Vol. 2. — P. 257–264.

Poole R. J., Budhiraja B., Cain A. R., Scott P. A. Emulsification using elastic turbulence // J. Non-Newton. Fluid Mech. — 2012. — Vol. 177, No. 78. — P. 15–18.

Shahmardi A., Zade S., Ardekani M. N., Poole R. J., Lundell F., Rosti M. E., Brandt L. Turbulent duct flow with polymers // J. Fluid Mech. — 2019. — Vol. 859. — P. 1057–1083.

Slutsky M., Steinberg V. Effective mixing and emulsification of very viscous substances by elastic turbulence // Report on the Horowitz Foundation Grant 3355. — Rehovot, Israel: Weizmann Inst. Sc. — 2005.

Steinberg V. Elastic turbulence: an experimental view on inertialess random // Flow. Annu. Rev. Fluid Mech. — 2021. — Vol. 53. — P. 27–58.

Thomases B., Shelley M., Thiffeault J.-L. A Stokesian viscoelastic flow: transition to oscillations and mixing // Phys. D: Nonlinear Phenomena. — 2011. — Vol. 240. — P. 1602–1614.

Traore B., Castelain C., Burghelea T. Efficient heat transfer in a regime of elastic turbulence // J. Non-Newton. Fluid Mech. — 2015. — Vol. 223. — P. 6.

Vaithianathan T., Collins L. R. Numerical approach to simulating turbulent flow of a viscoelastic polymer solution // J. Comput. Phys. — 2003. — Vol. 187. — P. 1–21.

Vaithianathan T., Robert A., Brasseur J. G., Collins L. R. An improved algorithm for simulating three-dimensional, viscoelastic turbulence // J. Non-Newtonian Fluid Mech. — 2006. — Vol. 140. — P. 3–22.

Whalley R., Abed W. M., Dennis D. J. C., Poole R. J. Enhancing heat transfer at the micro-scale using elastic turbulence // Theor. Appl. Mech. Lett. — 2015. — Vol. 5. — P. 103–106.